LBNL-60512/CBP Note-736

# STUDIES OF E-CLOUD BUILD UP FOR THE FNAL MAIN INJECTOR AND FOR THE LHC*

M. A. Furman, LBNL, Berkeley, CA 94720-8211, USA†

## *Abstract*

We present a summary of recent simulation studies of the electron-cloud (EC) build-up for the FNAL MI and for the LHC. In the first case we pay particular attention to the dependence on bunch intensity $N_b$ at injection energy assuming the nominal bunch spacing $t_b = 19$ ns, and we focus on the dipole magnets and field-free regions. The saturated value of the average EC density shows a clear threshold in $N_b$ beyond which the beam will be approximately neutralized on average. For the case of the LHC we limit our discussion to arc dipoles at collision energy, and bunch spacings $t_b = 25$ ns or $t_b = 75$ ns. The main variables exercised in this study are $N_b$ and the peak value of the secondary emission yield (SEY) $\delta_{\max}$. For $t_b = 25$ ns we conclude that the EC power deposition is comfortably below the available cooling capacity of the cryogenic system if $\delta_{\max}$ is below $\sim 1.2$ at nominal $N_b$. For $t_b = 75$ ns, the EC power deposition is insignificant. As a byproduct of this exercise, we reach a detailed understanding of the significant role played by the backscattered secondary electrons. This article summarizes the results, an slightly extends the discussions, presented in Refs. 1 and 2.

## INTRODUCTION

Two recent articles describe the simulated EC build-up for the EC in the LHC arc dipoles at beam energy $E_b = 7$ TeV [1] and a similar investigation for the proposed FNAL Main Injector (MI) upgrade at $E_b = 8$ GeV[1] in a bending magnet and in a field-free region [2]. These simulations were carried out with the EC build-up code POSINST, a 2D not-self-consistent code in which the beam is a prescribed function of space and time while the electrons, represented by macroparticles, are fully dynamical [3–6]. The code embodies a detailed probabilistic model for secondary electron emission (SEE), whose parameters were obtained from fits to laboratory measurements of the SEY function $\delta(E_0)$, where $E_0$ is the incident electron energy, and the secondary emission energy spectrum (SEES) $d\delta/dE$ [5, 6]. The code has been successfully validated by benchmarks against dedicated measurements of the electron flux at the vacuum chamber walls at the APS [7] when it was run with a positron beam, and at the PSR [8]. Although the agreement between simulations and measurements in these two cases was satisfactory, it should be kept in mind that certain parameters pertaining to SEE, used as input to the simulations, are rarely, if ever, precisely known in advance for any given case. This is to a large extent a consequence of the fact that some such parameters, particularly the peak SEY $\delta_{\max}$, are not static, but rather evolve as a result of the surface conditioning process as a natural consequence of machine operation or changes in vacuum conditions. Thus the above-mentioned validation exercises can be considered fruitful if the agreement between simulation and measurement requires adjusting only a few parameters within a narrow and reasonable range values. In this sense, the two above-mentioned benchmarks against measurements at the APS and PSR were successful.

For the case of the LHC we have carried out a fairly extensive sensitivity analysis of our results against variations in the numerical computation parameters as well as against variations in the model parameters. As a byproduct, we find good agreement with the results obtained at CERN with the code ECLOUD provided the models employed for the SEY are similar [9]. For the case of the MI, a comparable sensitivity analysis has yet to be carried out, and our results represent only an initial step in what will be a more extensive analysis. The simulated EC build-up for the two machines, particularly the threshold behavior as a function of $N_b$, show strong qualitative differences which we intend to explain in the near future [10].

A newer 3D self-consistent code, WARP/POSINST, is being developed in our group and will be applied to investigate the effects of the EC and the beam under their mutual and simultaneous influence [11]. This code is being systematically validated against other simulation codes and against experiments at the HCX facility at LBNL [12].

## LHC

The main concern from the EC at the LHC is an excessive power deposition by the electrons striking the walls of the chamber. Since the LHC cryogenic system was designed before the discovery of the EC effect, its specifications did not take into account this extra source of power deposition, which must be dissipated if the LHC is to function as nominally specified. Consequently, much effort has been devoted to estimate the EC power deposition as accurately as possible, and to devise mitigating mechanisms if necessary [13]. Another important concern, namely slow emittance growth, has been recently raised [14]; we will not

---

* Work supported by the US Department of Energy under contract DE-AC02-05CH11231 and by the US-LHC Accelerator Research Project (US-LARP).

† mafurman@lbl.gov

[1] Owing to a misunderstanding, we chose 8 GeV as the MI injection energy, when in fact it is 8.9 GeV. This 10% error has negligible effect on our results.

address this latter issue here. Since the LHC beam needs to be stably stored for 10-20 hrs, these two issues (and many others, of course) need to be well understood and controlled in order to maximize integrated luminosity.

Our main results are summarized in Fig. 1, which shows the simulated average linear power deposition $d\bar{P}/dz$ vs. $N_b$ for various values of $\delta_{\rm max}$. For the cryogenic system to be able to dissipate the EC power deposition, the conditions must be such that $d\bar{P}/dz$ is below the dotted lines labeled "ACC" [15]. For each value of $\delta_{\rm max}$, there are 3 sets of data corresponding to 3 different models of SEE. The results show a sensitivity not just to the SEY, but also to the SEES. If the rediffused component of the spectum is artificially set to zero while the true secondary and backscattered components are scaled up so that $\delta_{\rm max}$ remains fixed (traces labeled "NR"), $d\bar{P}/dz$ is roughly cut in half relative to the model with the full SEES, which includes the rediffused component (traces labeled "R"). The parameters of model "R" used in the simulation were obtained from fits to copper data.[2] The results for cases "R" and "NR" were obtained with our code POSINST, while the results labeled "LTC40" were obtained with the CERN code ECLOUD. One sees that the traces "NR" and "LTC40" are in good agreement, as expected, since in these two cases the SEE models are approximately the same (they both exclude rediffused electrons) [9]. The explanation for the relatively large contribution of the rediffused electrons ($\sim 100\%$ increase in $d\bar{P}/dz$ for $\sim 10\%$ increase in the rediffused component) is given in Sec. IV of Ref. 1. A key component of the explanation is the large bunch spacing, which allows more than one generation of secondary electrons to cross the chamber between any two bunch passages.

Figure 2 shows $d\bar{P}/dz$ for $N_b = 1 \times 10^{11}$ as a function of $\delta_{\rm max}$, exhibiting a clear threshold at $\delta_{\rm max} \simeq 1.2$. The values for $d\bar{P}/dz$ shown in Figs. 1 and 2 are computed from a first-batch injection into an empty chamber; steady-state values for $d\bar{P}/dz$ are $\sim 40\%$ larger than these [1]. For this reason, we conclude that a reasonable condition for $d\bar{P}/dz$ not to exceed the available cooling capacity of the cryogenic system is $\delta_{\rm max} \lesssim 1.2$. The beam conditioning time required to reach such a value of $\delta_{\rm max}$ remains to be computed in detail. This issue if further discussed below.

If the bunch spacing is 75 ns instead of 25 ns, $d\bar{P}/dz$ (not shown) is comfortably below the available cooling capacity of the cryogenic system for almost any realistic conditions, hence in this case the EC is not expected to pose any operational limitations to the LHC vis-à-vis the EC power deposition.

The stability of these calculations against changes in computational parameters has been verified to a substantial degree, and the sensitivity to model parameters reasonably well explored. However, uncertainties remain, primarily arising from the lack of detailed knowledge of the percentage of rediffused electrons and the value of $\delta(0)$. Such uncertainties could be removed to some extent by detailed measurements of the SEY and SEES for actual samples of the LHC beam screen copper surface; however, it should be kept in mind that some uncertainties will inevitably remain as a result of the expected conditioning process once the LHC starts storing beam.

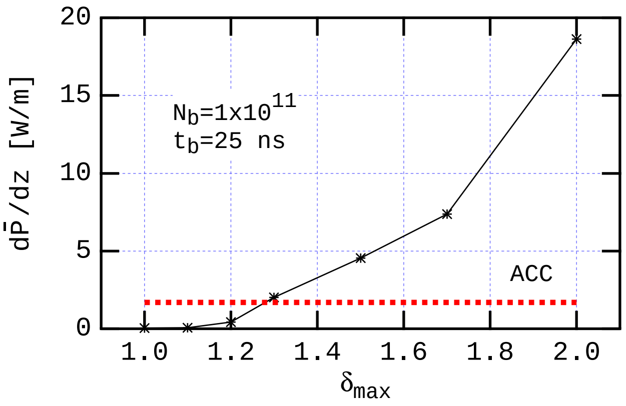

Figure 2: Average power deposition in an LHC arc dipole magnet vs. $\delta_{\rm max}$ for $N_b = 1 \times 10^{11}$. "ACC:" available cooling capacity of the cryogenic system.

## MAIN INJECTOR

A proposed upgrade of the MI calls for an increase in $N_b$ by a factor $\sim 5$ from its present value of $6 \times 10^{10}$, plus a possible change in RF frequency. The upgrade is intended to use the MI as a high-intensity neutrino source (HINS) [16]. Unlike the LHC, the cycle time of the machine (injection, ramping, fast extraction) is quite short, $\lesssim 1$ s, hence the main concerns raised by the upgrade pertain not to emittance growth but to the development of beam haloes which might lead to excessive activation upon beam extraction [17]. Investigations of the EC at the MI [18] and the Tevatron [19–21] show a high likelihood of the presence of an EC at high beam intensity, although direct electron detection is not yet available.[3]

A preliminary simulation of the EC build-up at the MI [2] at injection energy shows a strong threshold effect in the average electron density $\rho_e$ as a function of $N_b$, as seen in Fig. 3. The density $\rho_e$ rises by $\sim 5$ orders of magnitude beyond threshold, reaching a level where the proton beam is essentially neutralized on average, and leading to a contribution $\sim +0.05$ to the space-charge tune shift. Above threshold, the time development of the EC build-up is exponential with a risetime of $\sim 1$ $\mu$s (see Fig. 4).

The actual parameter that controls the severity of the EC is the effective SEY $\delta_{\rm eff}$, namely the average SEY over all electrons striking the wall during any relevant time interval. If $\delta_{\rm eff} > 1$, the EC is strong, and if $\delta_{\rm eff} < 1$ the EC is

---

[2] In our simulations we used old data sets for the SEY and SEES that might not correspond to the actual LHC beam screen surface. New measurements for such a material would be highly desirable.

[3] Two electron detectors, one each in the MI and the Tevatron, were recently installed and are expected to begin data acquisition during the current run.

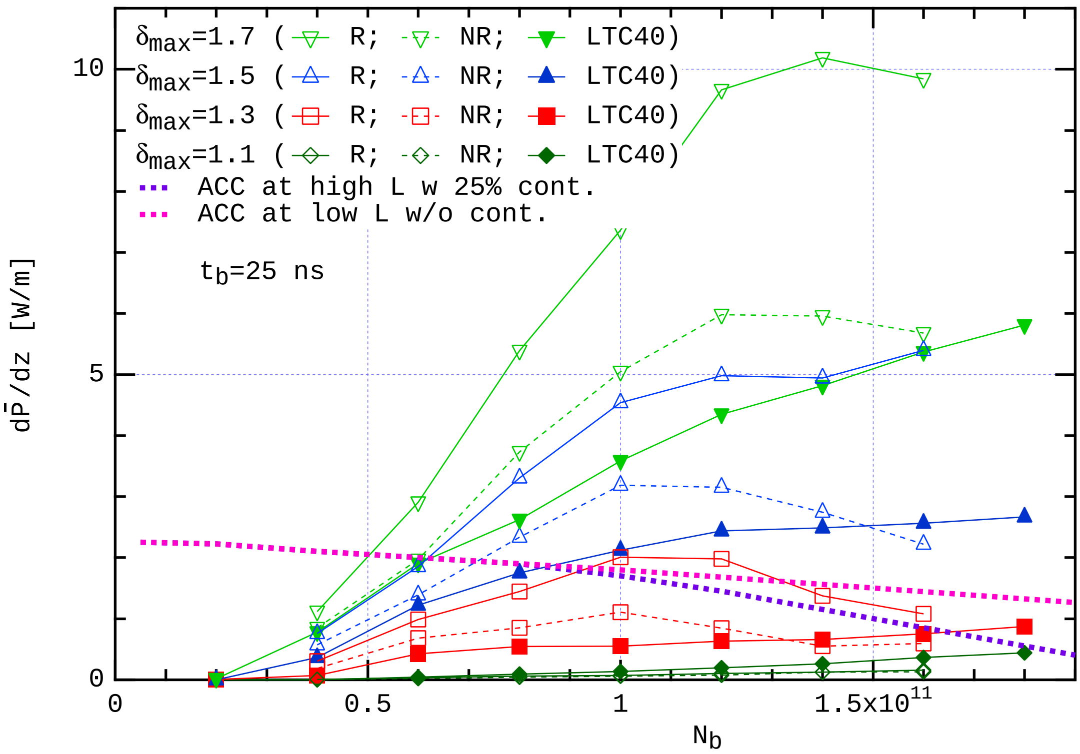

Figure 1: Average power deposition per unit length of chamber in an LHC arc dipole magnet vs. $N_b$ for $t_b = 25$ ns. "R:" full SEES; "NR:" SEES without the rediffused component; "LTC40:" results from Ref. 9; "ACC:" available cooling capacity of the cryogenic system at high luminosity with 25% contingency, or at low luminosity with no contingency.

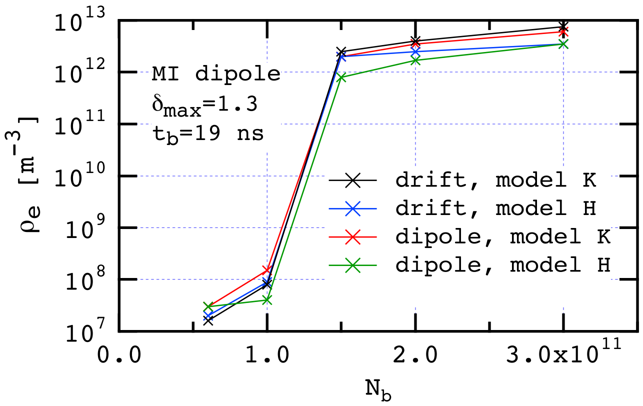

Figure 3: Average electron density in steady state for the MI vs. $N_b$ assuming $\delta_{\max} = 1.3$. This choice for $\delta_{\max}$ is meant only as an initial step in a more comprehensive analysis yet to be carried out. Models "H" and "K" represent two choices for certain details of the SEES. Model "H" for the MI is the same as model "R" for the LHC (Fig. 2).

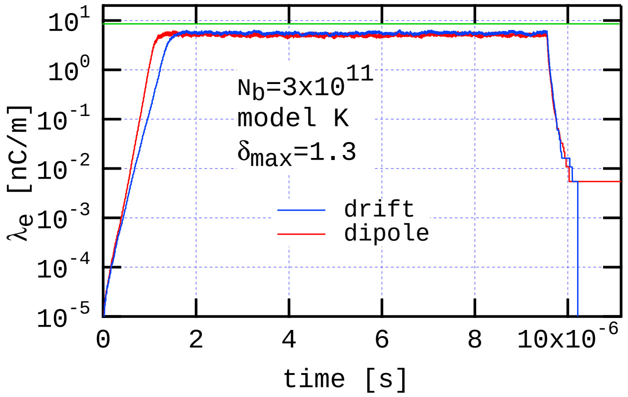

Figure 4: Build-up of the average EC line density during one revolution in the MI for $N_b = 3 \times 10^{11}$. The horizontal green line represents the average beam neutralization level, given by $\lambda_b = eN_b/s_b = 8.5$ nC/m, where $s_b = 5.6$ m is the bunch spacing (or RF wavelength, in this particular case).

weak or nonexistent. These two possibilities were explicitly shown to happen in the MI above and below threshold, respectively [2]. Although $\delta_{\rm eff}$ has a monotonic dependence on $\delta_{\max}$, it is not easy to compute a priori; it is

obtained as a byproduct of the simulation, as it requires an average over all electron wall-collision events in the chamber during the chosen time interval.

## CONDITIONING

When a metallic surface is continuously bombarded with electrons, its SEY steadily decreases. For an electron dose $D$ in the range $10^{-4} \lesssim D \lesssim 1$ C/cm$^2$, controlled bench experiments and measurements in vacuum show that the peak SEY $\delta_{\max}$ roughly follows a logarithmic dependence with dose,

$$\delta_{\max} \simeq d_1 - d_2 \log D \tag{1}$$

so that $\delta_{\max} \sim 1$ when $D \sim 1$ C/cm$^2$ ($d_1$ and $d_2$ are material-dependent positive constants that are not critical for the present discussion) [22, 23]. This implies that the EC in storage rings is self-conditioning: the very electrons from the cloud gradually condition the chamber surface until $\delta_{\max}$ is so small that the effect becomes innocuous. The important question, of course, is how long it takes for this beam conditioning process to bring the SEY down to such a level. This beam conditioning effect has been clearly observed in storage rings in which the EC is initially present [24, 25]

Figure 5 shows sample results for the simulated bombardment rate, i.e., electron flux at the wall $J_e$, for the LHC and MI as a function of $N_b$ assuming $\delta_{\max} = 1.3$. The turnover seen in the case of the LHC is due to the fact that for large $N_b$ the electrons strike the walls of the chamber with a typical energy larger than $E_{\max}$, i.e., the value at which $\delta(E_0)$ has a maximum. As a result, as $N_b$ increases above $\sim 1 \times 10^{11}$, the effective SEY decreases, hence so does the average electron density in the chamber, and hence so does $J_e$. The peak bombardment rate occurs just below the nominal beam intensity, a curious coincidence. For the MI, the turnover has not been reached even for $N_b = 3 \times 10^{11}$, possibly because the larger bunch length of the MI ($\sigma_z = 75$ cm) leads to a weaker beam-electron kicks than for the LHC ($\sigma_z = 7.7$ cm).

## DISCUSSION

While we have ascertained the stability of our LHC results against variations in computational parameters, and we have reasonably well understood the sensitivity to several physical parameters, we have not yet carried out such validation exercise for the MI, particularly the sensitivity to $\delta_{\max}$. For the case of the LHC dipoles, the electron density (not shown) has a qualitatively similar dependence on $N_b$ as $d\bar{P}/dz$ does (Fig. 1), with a threshold $N_{b,\mathrm{th}} \sim 2 \times 10^{10}$ and an approximately linear rise in $(N_b - N_{b,\mathrm{th}})$ for $N_b > N_{b,\mathrm{th}}$. The striking qualitative difference with the results for the MI, for which $\rho_e$ rises suddenly for $N_b > N_{b,\mathrm{th}} \sim (1-1.5) \times 10^{11}$ and is quickly followed by saturation, demands an explanation. It is almost certainly the case that the large bunch spacing in the LHC compared with the MI plays a significant role (bunch length may also be important). We expect to address these issues in the near future [10].

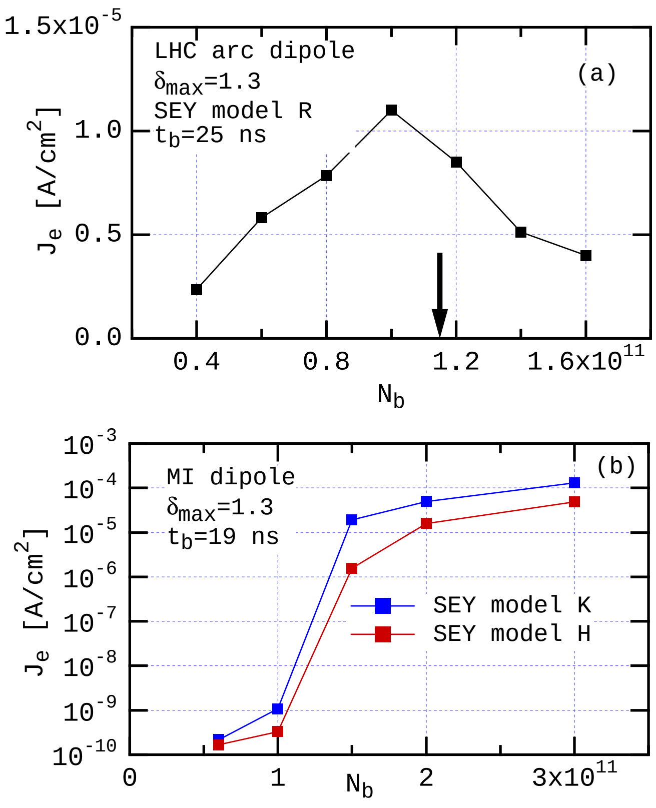

Figure 5: Average electron flux at the wall for the choice $\delta_{\max} = 1.3$. (a) LHC arc dipole magnet at beam energy $E_b = 7$ TeV; (b) MI dipole at $E_b = 8$ GeV. The models refer to specific parameter choices for the SEY and SEES. Model "K" for the MI is the same as model "R" for the LHC. The arrow in (a) indicates the nominal bunch intensity, $1.15 \times 10^{11}$.

A conservative rule of thumb is that EC effects become negligible when $\delta_{\max} \sim 1$, which, as mentioned above, requires a dose $D \sim 1$ C/cm$^2$. Taking this rule of thumb as a very rough guide for the beam conditioning process, the results in Fig. 5 imply a beam conditioning time of several centuries for the MI at $N_b = 6 \times 10^{10}$, a few hours at $N_b = 3 \times 10^{11}$, and tens of hours for the LHC at $N_b = 1 \times 10^{11}$. Of course, this estimate is extremely simplistic because, as conditioning progresses, $\delta_{\max}$ decreases, hence so does the electron flux at the wall, hence the process gradually slows down. On the other hand, an innocuous EC might be achieved for values of $\delta_{\max}$ somewhat larger than unity. A further complication in the conditioning time estimates is that the three components of the SEES do not seem to condition at the same rate for a given dose; indeed, recent data [26] for cold copper indicates that the elastically backscattered component does not condition at all for very low values of incident electron energy.

## ACKNOWLEDGMENTS

I am indebted to V. Baglin, A. Chen, W. Chou, R. Cimino, W. Fischer, K. Y. Ng, J.-F. Ostiguy, D. Schulte, A.

Wolski, P. Yoon, X. Zhang and F. Zimmermann for valuable discussions. Work supported by the US DOE under contract DE-AC02-05CH11231, by the US-LHC Accelerator Research Program (LARP), and by DOE Office of Science Undergraduate Laboratory Internship (SULI) Program.

## REFERENCES

[1] M. A. Furman and V. H. Chaplin, PRST-AB **9** 034403 (2006).

[2] M. A. Furman, LBNL-57634/CBP-Note-712/FERMILAB-PUB-05-258-AD, June 28, 2005, to be published in the New Journal of Physics.

[3] M. A. Furman and G. R. Lambertson, Proc. "MBI-97" (KEK, 15—18 July 1997; Y. H. Chin, ed.), KEK Proceedings **97-17**, Dec. 1997, p. 170.

[4] M. A. Furman, LBNL-41482/CBP Note 247/LHC Project Report 180, 20 May 1998.

[5] M. A. Furman and M. T. F. Pivi, PRST-AB **5**, 124404 (2003).

[6] M. A. Furman and M. T. F. Pivi, LBNL-52807/SLAC-PUB-9912, June 2, 2003.

[7] M. A. Furman, M. Pivi, K. C. Harkay and R. A. Rosenberg, Proc. PAC01, p. 679.

[8] M. A. Furman and M. Pivi, Proc. PAC01, p. 707.

[9] F. Zimmermann, LTC meeting #40, CERN, 6 April 2005, http://edms.cern.ch/lhc_proj/plsql/lhcp.page?p_number =7700

[10] M. A. Furman, in progress.

[11] J.-L. Vay, paper THAW01, these proceedings.

[12] A. Molvik, paper THAW02, these proceedings.

[13] Many historical and current references can be found in Ref. 1. A particularly valuable resource is the CERN website on EC in the LHC, http://ab-abp-rlc.web.cern.ch/ab%2Dabp%2Drlc%2Decloud/

[14] E. Benedetto, paper TUAX03, these proceedings.

[15] F. Zimmermann, LHC MAC mtg. #17, June 2005; http://mgt-lhc-machine-advisory-committee.web.cern.ch/mgt-lhc-machine-advisory-committee/lhcmac17/ClosedSession/Zimmermann.pdf

[16] A. Marchionni, paper MOCP01, these proceedings.

[17] R. Zwaska, paper WEAZ02, these proceedings.

[18] R. Zwaska, paper THAW05, these proceedings.

[19] F. Zimmermann, FNAL BEAMS-DOC-304-v1, 2002.

[20] X. Zhang, FNAL BEAMS-DOC-1991, 2002.

[21] X. Zhang, FNAL BEAMS-DOC-2263, 2005.

[22] R. E. Kirby and F. K. King, NIMPR A **469**, 1-12 (2001).

[23] V. Baglin, I. Collins, O. Gröbner, B. Henrist, N. Hilleret and G. Vorlaufer (talk given by N. Hilleret), Proc. "Two-stream 2001," (KEK, Sept 11–14, 2001).

[24] J. M. Jiménez, G. Arduini, P. Collier, G. Ferioli, B. Henrist, N. Hilleret, L. Jensen, K. Weiss and F. Zimmermann, LHC Project Report 632, 8 April 2003.

[25] R. J. Macek, A. A. Browman, M. J. Borden, D. H. Fitzgerald, R. C. McCrady, T. Spickermann and T. J. Zaugg, Proc. "ECLOUD04," (Napa, California, April 19-23, 2004; M. Furman, S. Henderson and F. Zimmermann, eds.), CERN Yellow Report CERN-2005-001/CARE-Conf-05-001-HHH/LBNL-56372/SNS-10400000-TR0024-R00, p. 63.

[26] R. Cimino and I. R. Collins, Appl. Surface Sci. **235**(1), pp. 231–235, July 2004.

## DISCLAIMER